Universiteit Leiden

Opleiding Informatica

Image optimization, feature extraction and
classification in Neurobiology:

"Dendritic spines under stress"

T. Vermeulen
J.F.J. Oosterhof

Supervision:
F.J. Verbeek, Leiden Institute of Advanced Computer Science
C. Fitzsimons, Leiden/Amsterdam Center for Drug Research

BACHELOR THESIS

Leiden Institute of Advanced Computer Science (LIACS)

Leiden University
Niels Bohrweg 1
2333 CA Leiden
The Netherlands

Abstract

In neurons, the dendritic structure is sensitive to changes in the environment. Several treatments have been known to create changes in dendritic structure. 3D confocal images have been used before to evaluate and quantify changes in dendritic structure. In this research, specific treatment with a lentivirus in vivo lead to green fluorescent protein expression. Moreover, the lentiviruses were engineered to knock down the glucocorticoid receptor. Based on these biological features our work created a method for analysing dendritic spines in a semi-automated fashion, which involves the use of a confocal laser scanning microscope, deconvolution, the NeuronStudio software, statistical analysis using SPSS and the WEKA data mining tool. This research showed that the glucocorticoid receptor knockdown causes significant morphological changes in spine structures in the hippocampus of mouse brains. These changes indicate more spine maturation.

Introduction

A neuron is a structural and functional unit of the brain, consisting of a cell soma (cell body), one or more dendrites and one axon ending in axon terminals [1]. The neuron is connected to other neurons, forming a giant complex network. The cerebral cortex consists of more than ten billion neurons [2]. Dendrites are the branched projections of a neuron that act to conduct the electrochemical stimulation received from other neural cells to the cell body, or soma, of the neuron from which the dendrites project. Dendritic spines, tiny growths on dendrites, increase the richness of connections among neurons. The excitability of the neuron is directly related to the amount of dendrites and the amount and types of spines on it [3]. Three different types of spines can be structurally distinguished: stubby, mushroom and thin [1].

A young neuron has short thick dendrites and develops into a complex network of smaller dendrites, increasing the surface area. During development of the neuron, an excess of spines is formed on the dendrites. Those spines making connections with other neurons will thicken and shorten, the unconnected dendrites will elongate and finally drop off [2]. It is believed that abnormal formation of the spines is related to learning disorders [2], which makes it interesting to do research on. In this way we get a better understanding of the underlying morphological changes of such learning disorders.

Contrary to the long held dogma, neurogenesis, the generation of new nerve cells, occurs in the adult mammalian brain. Neurogenesis occurs mainly in two areas of the adult brain in mammals: the dentate gyrus (DG) of the hippocampus, and the subventricular zone (SVZ), along the ventricles.

The dentate gyrus (DG) plays an important role in learning and long time memory formation [4], [5]. It is one of the few brain structures currently known to have high rates of neurogenesis during adult life and thus sensitive to changes in mechanisms controlling it (neurogenesis) [6]. The high rate of neurogenesis in the DG and it's role in learning and memory formation are closely related. New neurons are constantly generated from a resident population of stem cells located in the border of the hilus and granule cell layer of the dentate gyrus. These neural stem cells (NSCs) are defined by their ability to undergo multipotent differentiation into major cell lineages, including neurons and astrocytes, as well as by their capacity to produce identical cells (self-renew) [7], [8]. In vitro, NSCs or stem-like cells have been isolated from the dentate gyrus [9]. A recent in vivo fate analysis study of SRY-related HMG-box transcription factor SOX2 transgenic mice showed that a single SOX2-positive cell can generate neurons, astrocytes, and identical SOX2+ cells at single-cell level, providing the first in vivo evidence of the multipotent and self-renewal properties of NSCs in the adult hippocampus [10].

Several receptors are believed to influence the development of newborn cells, including the glucocorticoid Receptor (GR) [11]. Knockdown of GR can lead to a marked change in the relative location of newborn cells within the pre-existing granule cell layer (GCL) and most likely can promote neuronal differentiation [12], [13].

This research is based on the comparison between normal mouse brains and the brains of mice after GR knockdown in terms of the morphology of the dendrites and in particular its spines in the hippocampus of the brains. In order to perform this comparison 3D images of brain samples are acquired using a confocal laser scanning microscope (CLSM).

To avoid possible bias and to enable the analysis of large quantities of data, the image analysis is done in a semi-automated fashion. The NeuronStudio software (NS) as developed by the Computational Neurobiology and Imaging Centre in New York [14] is able to automatically detect dendrites and spines in 3D images. This ensures all images are handled in exactly the same way.

The output of NeuronStudio can be further analysed to discover certain features of the microscopic images, like the amount of a specific type of spine per length unit of the dendrite. In this way a large data set with features of the images is acquired. Using data mining [15], hidden patterns can be discovered out of this data, which are often hard to see without such tools. Using these patterns a classifier can be created that is able to distinguish between a normal and a GR knockdown neuron.

Materials and methods

Research groups

As a model for this research, samples of the hippocampus of mouse brains were used. Samples of one and five week old brains of healthy mice were used as control groups, C1 and C2 respectively. The treatment group, one week old, received a specific treatment with a lentivirus leading to the knockdown of the GR.

To knockdown the GR in neuronal progenitor cells (NPC) and their neurogenic progeny in vivo, lentivirus suspensions were delivered to the DG of the adult mouse hippocampus by stereotaxic injections to the hilar region [13].

Sampling

Samples of 5 different animals have been used: two animals for C1, one for C2 and two for the treatment group. Each sample was stained using anti-green fluorescent protein (GFP) antibodies with a 488nm excitation wavelength. The image acquisition was done six months after the sampling.

Image acquisition

An inverted Nikon TE 2000 confocal microscope with Nikon EZ-C1 software has been used in combination with a GFP-488 excitation laser. A 60x oil immersion lens (NA, 1.25; Nikon) was used for an optimal magnification. A 20x lens was used to create larger scale images in order to search for interesting sections of the samples.

Although it is possible to use the microscope manually to view and navigate through samples, the microscope can be completely software-operated (Nikon EZ-C1). This includes scrolling to different sections of the sample, making 2D as well as 3D images and changing image acquisition settings. Creating 2D images is quick and can be used to navigate through the sample. To create 3D images the user needs to specify the x, y and z coordinates of the desired section of the sample. The software then creates a 3D image consisting of multiple images in the x/y plane along the z-axis. In the software this is referred to as creating a Z-stack.

Within the software several settings can be adjusted that influence the quality and intensity of the acquired image and these have to be set properly. The most important settings are the pixel dwell time, pixel size, pinhole size, laser power and laser gain [16], because of their big effect on the resulting image.

Deconvolution

Because of background noise, Huygens Essential (HE) deconvolution software [17] from SVI B.V. was used to improve the quality of the acquired microscopic images. Because of the underlying algorithms used in the NS software [14], better results can be expected with deconvolved images rather than the original ones.

HE provides three different modes for background estimation: lowest value, in/near object and widefield. With the lowest value mode, the image is searched for a 3D region with the lowest average value. The object mode searches the neighbourhood around the voxel with the highest value for a planar region with the lowest average value. Finally, with the widefield mode the image is searched for a 3D region with the lowest values to ensure that the region with the least amount of blur contributions is found [18]. Each mode

will calculate an average background level which can be manually compared to average values of specific regions of the image by using the Twin Slicer tool.

In HE estimating the background is part of the deconvolution procedure. Depending on the selected background mode, the averaged background level will be estimated in a region far from or near the main objects in the image. This estimated value must be compared with what you actually consider background in the image [18].

NeuronStudio

NS is able to detect dendrites and spines using octree partitioning and voxel clustering[5]. By adjusting several settings like the voxel size, size requirements of dendrites/spines and the image signal threshold, the algorithm is able to detect the location of dendrites and classify its spines into one of the three preset categories: stubby, mushroom, thin (see figure 1). All basic data about the dendrites and spines that are found can be exported to a text file for further processing.
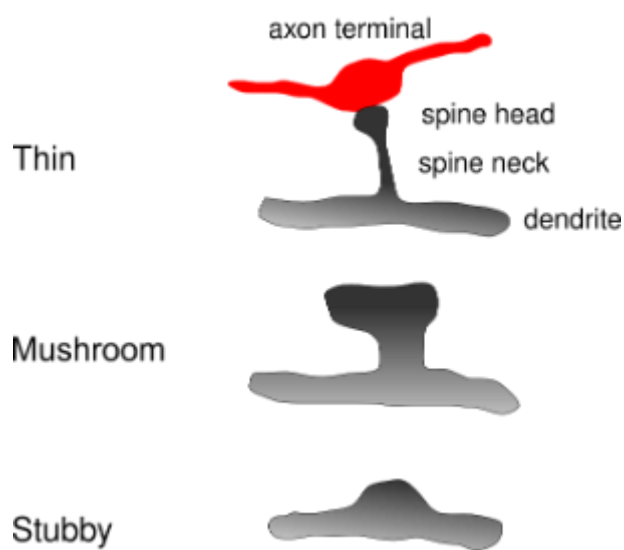

Figure 1: Different spine types

Weka

In order to analyse the data that is created with NS the Weka software package is used [19]. Weka supports several standard data mining tasks, more specifically, data pre-processing, clustering, classification, regression, visualization, and feature selection. All of Weka's techniques are predicated on the assumption that the data is available as a single flat file or relation, where each data point is described by a fixed number of attributes [20].

Results

Image segment selection

Because we are interested in acquiring images of dendrites within the hippocampus it is first necessary to locate the hippocampus within the sample. This is best done by using the 20x magnification lens and by controlling the microscope manually to retain a sense of overview and to make fast scrolling through the sample possible.

As the maximum resolution of the microscope used is close to the resolution needed to capture the shape and size of the spines, obtaining the highest possible quality images appeared vital for later image analysis. In order to achieve this it is necessary to carefully select the most viable dendrites in the samples. Selection criteria were a high signal intensity, visibility of spines, low level of background noise and a low density of dendrites. A low density of dendrites is desirable because later image analysis with NeuronStudio is hindered when dendrites are in close proximity of each other (see figure 3).
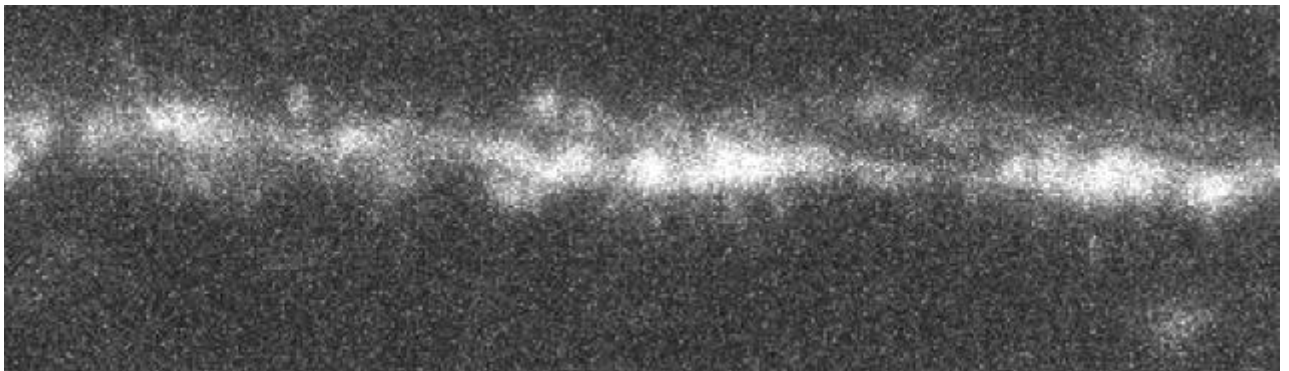

Figure 2: Example of an image of a dendrite with background noise and low intensity
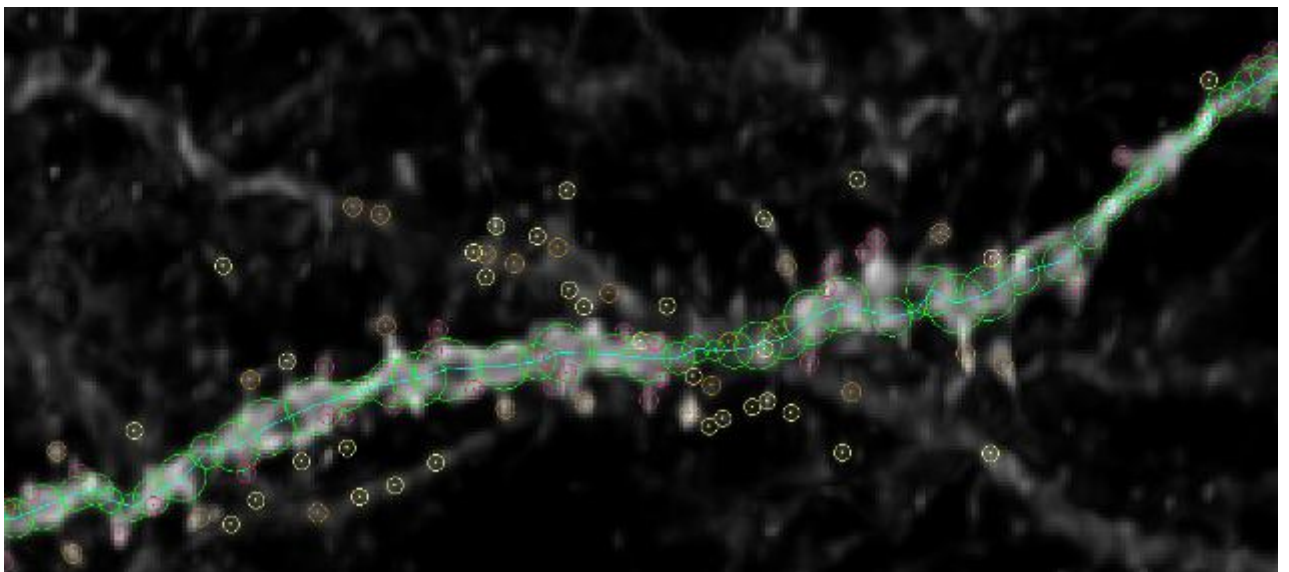

Figure 3: Example of an image where the dendrite is correctly classified by NS, but the spines are not
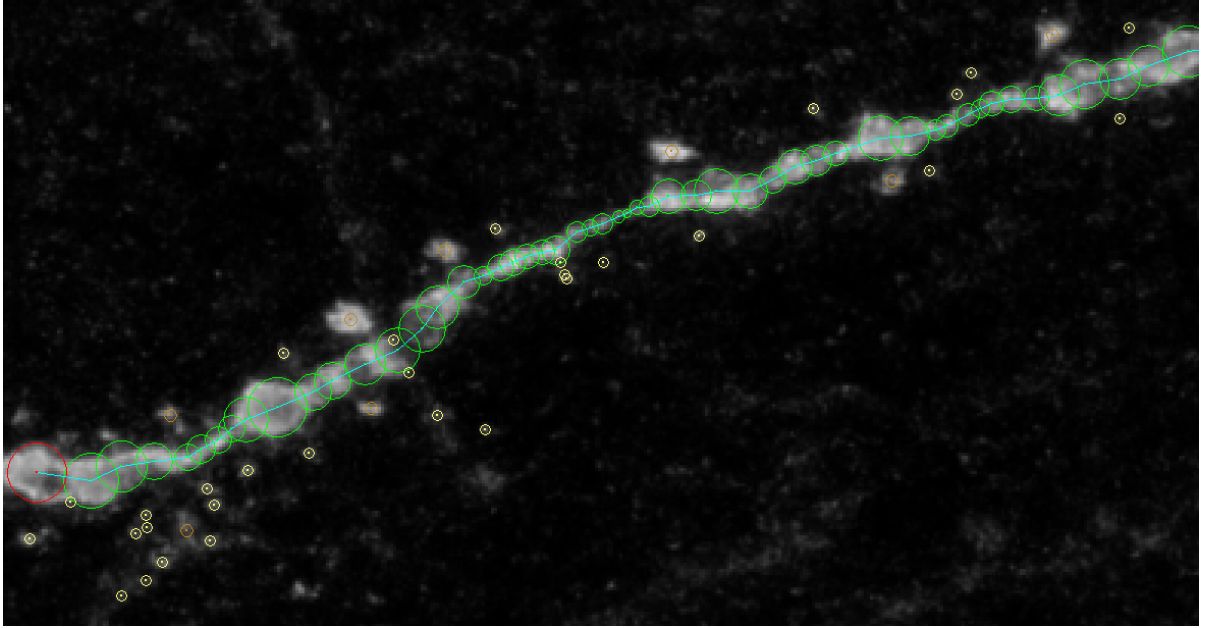
Figure 4: In this image the noise at the left bottom and the low signal intensity distort the result
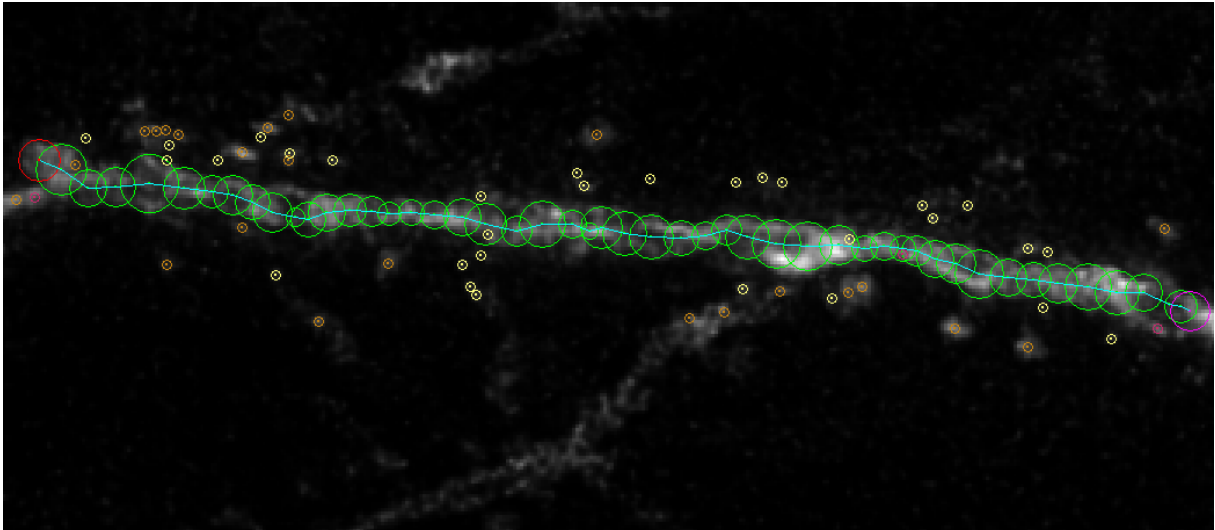

Figure 5: In this image most of the spines are classified incorrectly due to a low signal intensity and background noise caused by other dendrites
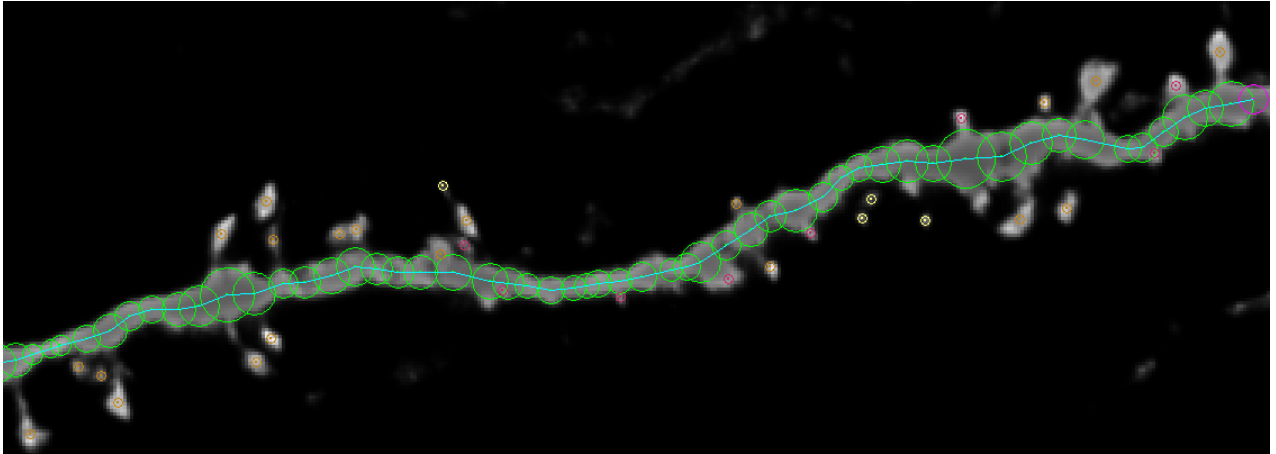
Figure 6: Example of an image with sufficient spine visibility. The image is successfully analyzed.

Problems with background noise and low signal intensity occurred with the majority of acquired images, which resulted in low spine visibility (see
figure 2, figure 4 and figure 5). Figure 6 shows an image where all search criteria are being met and the resulting analysis is successful. It seemed impossible to find a large number of dendrite segments that fully complied with these criteria, so we were forced to make compromises. Therefore, the predominant factor in segment selection was spine visibility considered as signal to background ratio. Some images with considerable background noise could still have good spine visibility as long as the signal intensity was high. Other images with low signal intensity were acceptable as long as the background noise was very low.

After locating the hippocampus we switched to a 60x magnification lens to find suitable dendrites. These dendrites are then evaluated further by switching the microscope to software mode and taking several 2D images of the segment at different settings. We tried to find settings that result in a good quality image, an image with a sufficient signal to background ratio. Only if such settings could be found for a specific dendrite a full 3D image (Z-stack) was taken. In this way repeating full 3D image acquisition for different settings can be avoided which saves time and helps to prevent bleaching of the sample. Bleaching is the deterioration of the sample by extensive exposure.

Acquisition settings

The main acquisition settings of the Nikon EZ-C1 software are the pixel dwell, pixel size, laser power, laser gain and pinhole size. It proved to be beneficial to adjust the settings per sample because with the same settings some samples would for example lack intensity as some samples would show too much background noise. We found that varying the laser gain and the pinhole size was sufficient to handle these differences between images. Laser power, pixel size and pixel dwell were kept constant for all images.

We used a voxel size of 75 by 75 by 100 nm which involves taking images with a pixel size of 75 by 75 nm at 100 nm intervals. It is important to take a small voxel size because the spine structures are very small and we want to get as much detail in the image as possible. Setting the voxel size even smaller was not useful as it would not actually add any detail to the image, because the maximum resolution of the microscope is reached. To prevent bleaching, we kept the laser power set at 35% of the maximum for all samples. The pixel dwell was always set at 3.0 microseconds. A larger pixel dwell time creates slightly better images but it is time consuming and it can cause bleaching.

The two pinhole sizes that we used where 30 nm and 50 nm, which are the smallest two pinhole sizes available to us. The smallest pinhole gives a sharper but weaker image, where the bigger pinhole gives a slightly more blurry image but captures more of the signal. We found it is best to use the small pinhole in most cases, but in some cases where the signal strength was low we used the bigger pinhole.

When setting the laser gain we tried to find a balance between good visibility of the spines and a low level of background noise. We first tried to find a laser gain that works using the small pinhole. If that did not result in a good quality image we tried to find a laser gain that works with the bigger pinhole. In cases where the laser gain could not be set so that a good quality image is taken, we did not take a full 3D image and moved on to another segment.

We have also made good use of the averaging function of the microscope, which takes multiple images of the same slice and then calculates an average over these images. In most cases using two or three averaging rounds removed a lot of background noise and made the image sharper. Increasing the number of averaging rounds above three did not have much effect on image quality, and we want to avoid doing too many rounds because of time-consumption and bleaching.

Deconvolution

The following microscopic parameters were used:

Microscope type:	confocal
Numerical aperture:	1.40
Lens immersion refr. index:	1.5150
Medium refractive index:	1.5150
X sample size (nm):	75
Y sample size (nm):	75
Z sample size (nm):	100

Table 1: Used microscope parameters

To set the right deconvolution parameters, we first compared the three methods for background level estimation by comparing background levels found with the Twin Slicer tool with the levels found by a certain estimation mode. For each different method, the area radius was tuned to get a result as close as possible to the value manually found with the Twin Slicer tool. In all test cases the object estimation mode with the default area radius of 0.5 micron performed best.

The signal to noise ratio was estimated at 20 by comparing its granularity to the images provided in the manual of HE and by checking the quality of the initial results of the deconvolution process. A total amount of 20 iterations with a quality threshold of 0.1 was enough to fulfil quality requirements for usage with NeuronStudio.

The optimised iteration mode algorithm detects if it hits upon a sub optimal result. If so, it switches back to the Classical mode to search for the optimum. That is why always starting with the optimised mode is highly recommended [18]. To reduce system memory usage, the image was automatically split into bricks while deconvolving.

Because we avoided bleaching of the samples during acquisition we did not use the bleaching correction function in the deconvolution software.
Final list of the deconvolution parameters:

Background estimation mode:	object (area radius 0.5 micron)
Relative background:	0
Maximum iterations:	20
Signal to noise ratio:	20
Quality threshold:	0.1
Iteration mode:	optimized/fast
Bleaching correction:	off
Brick layout:	auto

Table 2: Used deconvolution parameters

Figure 7 shows an image with good spine visibility, but with a considerable amount of background noise.
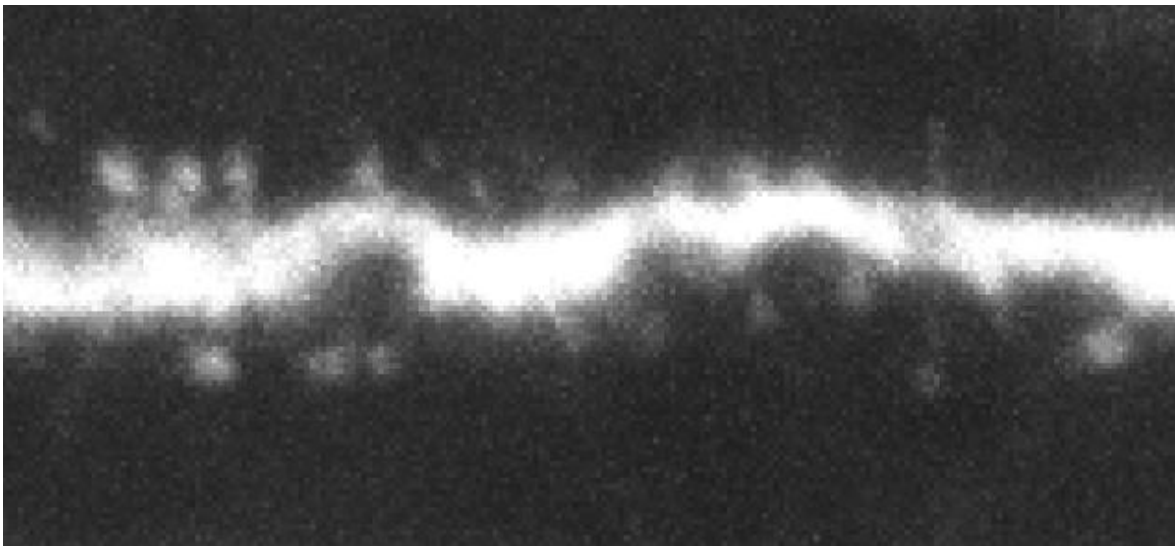
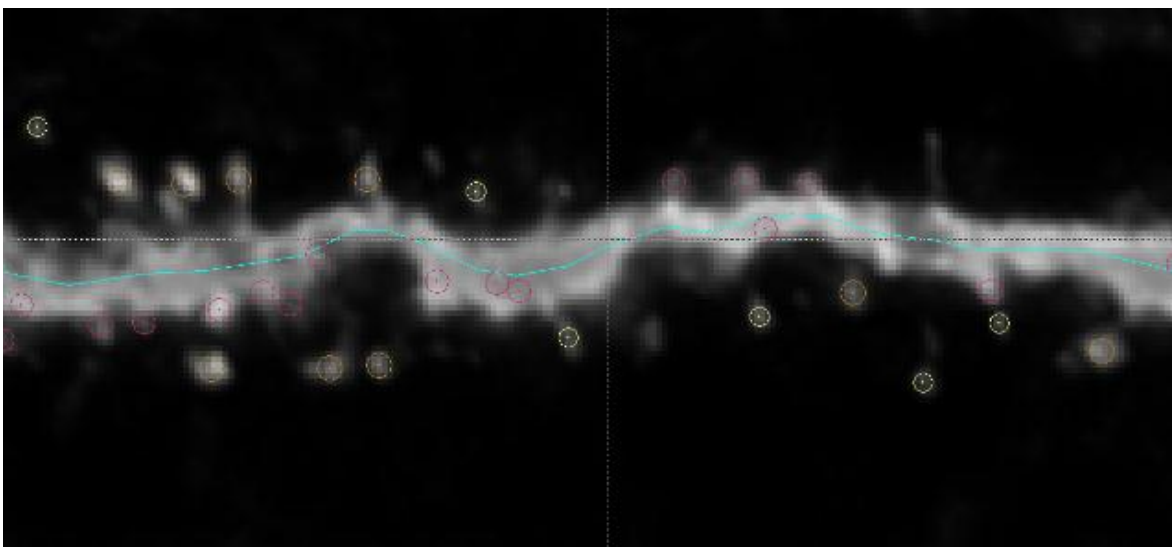Figure 8 shows the result after using deconvolution.

Figure 7: Original image

Figure 8: Deconvolved image and analyzed using NeuronStudio

NeuronStudio

The sequence of analysis with NeuronStudio starts with the user setting a seed somewhere within a dendrite. The software can then trace the dendrite starting from this point. If there are other dendrites visible in the segment, the seed can be moved and the tracing can be restarted. After tracing the dendrites in the image the software can detect spines that are located on these dendrites. Aside from setting the seed, the user can set the ROI (Region Of Interest), which forces the software to stay within a certain region of the image. We have used this in cases where only parts of the image were of good quality.

NS comes with pre-set analysis parameters that can be adjusted by the user. The most important parameters are concerned with shape requirements of the dendrites and spines and in particular classification requirements of different types of spines. When using the standard parameters of the software some spine detection and classification errors appear, meaning spine detection or classification is different than it would be if done manually. Manual analysis is done by studying the image using the 3D-viewer provided by NS where the user can, albeit rather arbitrarily, decide whether some shape is a spine and whether it is shaped as a mushroom, a stubby or a thin.

We found that the error rate can be reduced by adjusting the settings per sample. However, adjusting the settings to work well for one sample appeared to cause an increase in errors when used on other samples. Because our goal was to automate as much of the analysis procedure as possible, we chose to use the same settings for all images in order to avoid possible user bias, since manual analysis of the error rate is highly arbitrary.

After trying out different combinations of settings on a number of samples, the standard settings of NeuronStudio seemed to work best for our collection of samples. Below is a list of the settings that we used.

Dendrite detection

Attach ratio:	1.5
Minimum length:	3.0 µm
Neurite tracing threshold:	Dynamic

Spine detection and classification

Minimum height:	0.5 µm
Maximum height:	3.0 µm
Maximum width:	3.0 µm
Minimum stubby size:	10 voxels
Minimum non-stubby size:	5 voxels
Minimum head / neck ratio:	1.1
Minimum Thin ratio:	2.5
Minimum Mushroom size:	0.35 µm

Table 3: NeuronStudio settings

Final images

Using the image acquisition methods we described, we have gathered a total of 40 images each containing one or more segments of dendrites. Acquiring and analysing images using the described methods takes around 20 minutes per image. The majority of this time consists of image acquisition.

After deconvolving all of these 40 images we tried to analyse them with NS. For 30 images it was possible to get good results, meaning the analysis resulted in spine classifications that are correct for a large majority of the spines when checked manually.

Analysis of the other 10 images with NS created problems. In some of these cases NS was unable to trace the dendrite in the image, as it detected dendrites in segments of the image that contained only background noise (see figure 2). In many cases the dendrite was properly traced, but a large fraction of the spines were not detected or INCORRECTLY classified by NS (see figure 3, figure 4 and figure 5). These 10 images were discarded from further data analysis.

The 30 remaining images contained dendrites from the 3 different classes in the following amounts:

Control (C1):   10

Treatment (T):   12

5-week old control (C2): 8

These 30 dendrites have an average length of 145 µm each and contain on average 183 spines.

From the textfiles exported by Neuronstudio a number of attributes were derived for each dendrite. These attributes were used for further data analysis with Statistical Package for the Social Sciences (SPSS) and Weka. A list of attributes is given below.

Spine densities: (spines of a certain type per µm of dendrite)
- total spines per µm
- mushroom spines per µm
- stubby spines per µm
- thin spines per µm

Spine ratios: (spine counts of a certain type in relation to total spine counts)
- mushroom spine count / total spine count
- stubby spine count / total spine count
- thin spine count / total spine count

Spine shapes: (average shape measurements per spine type)
- average mushroom spine head diameter
- average mushroom spine neck diameter
- average mushroom spine spine length
- average mushroom spine head diameter / neck diameter
- average mushroom spine head diameter / spine length
- average thin spine head diameter
- average thin spine neck diameter
- average thin spine head diameter / neck diameter
- average thin spine spine length
- average thin spine head diameter / spine length
- average stubby spine diameter

- average stubby spine spine length
- average stubby spine head diameter / spine length

Dendrite measurements:
- dendrite thickness (the diameter of the dendrite)

Statistical analysis using SPSS

In the following figures the type refers to the three research groups: two control groups (c, c2) and one treatment group (t). The error bar above each bar indicates the standard error of the mean (SEM).

Spine type ratios

As figure 9 and figure 10 show, the treatment and second control group have a much higher mushroom/spine ratio and a much lower stubby/spine ratio than the first control group. This suggests that the spines of the treatment and second control group are in a more developed state [21].
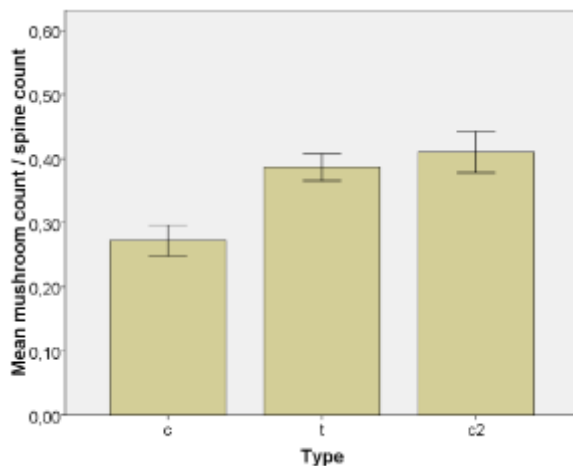

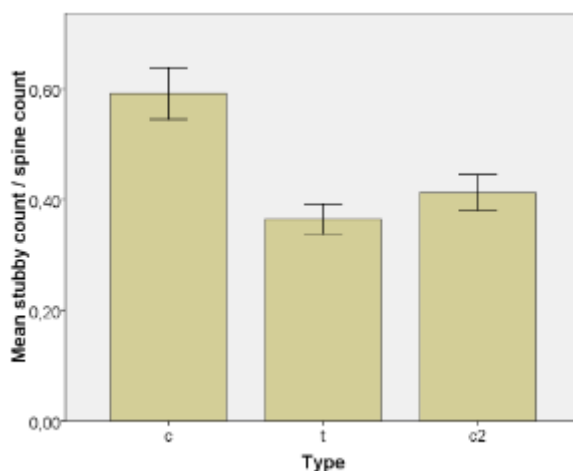**Figure 9: Ratio of mushrooms/total spine count per type**

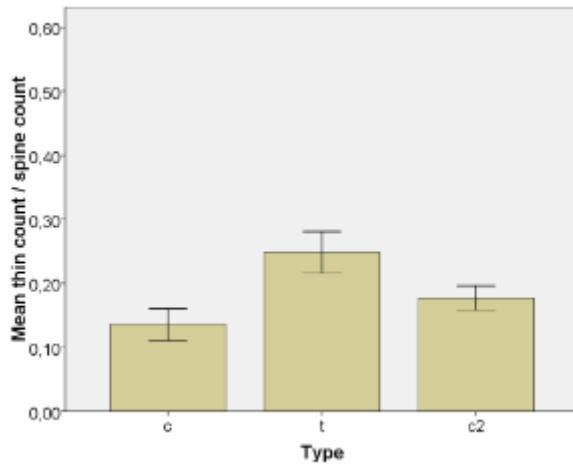**Figure 10: Ratio of stubbys/total spine count per type**

Figure 11: Ratio of thins/total spine count per type

Because thin spines can develop into mushroom spines [21], the high thin/spine ratio of the treatment group (see figure 11) indicates that the spines of this group are generally in a more active state of development compared to the control group. These thin spines can shorten and thicken, forming mushrooms, or elongate and finally drop off [2]. The high stubby/spine ratio of the first control group suggests that these spines are generally in an earlier state of development than the other groups. Both a low stubby/spine and thin/spine ratio for the second control group shows that this group generally consists of more matured spines than the other groups.

Spine densities

Figure 12 shows that the spine density is not significantly different between each research group (sig. 0,724).
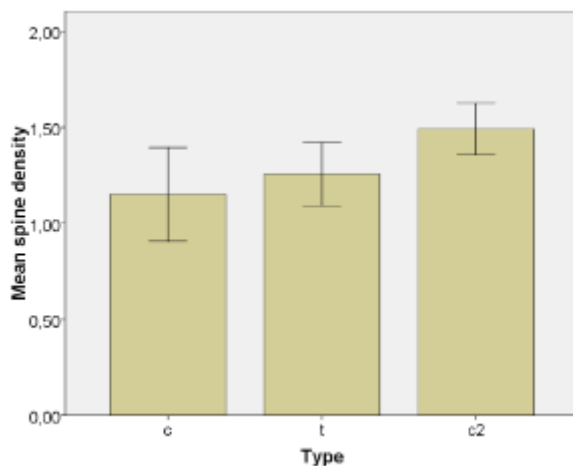

Figure 12: Mean spine density per type

Mushroom head/neck

Mushrooms with larger heads and thinner necks have been identified as being more mature [22]. As figure 13 and figure 14 show, the mushroom head/neck ratio is significantly lower (sig. 0,01) within the first control group due to an increased neck diameter. These results suggest that the mushrooms of the treatment and second control group are in a more mature state than those of the first control group, which has mushrooms with thicker necks.

Regarding the neck and head diameters of the mushroom spines, no significant differences exist between the treatment and second control group (sig. 0,713 and 0,125).
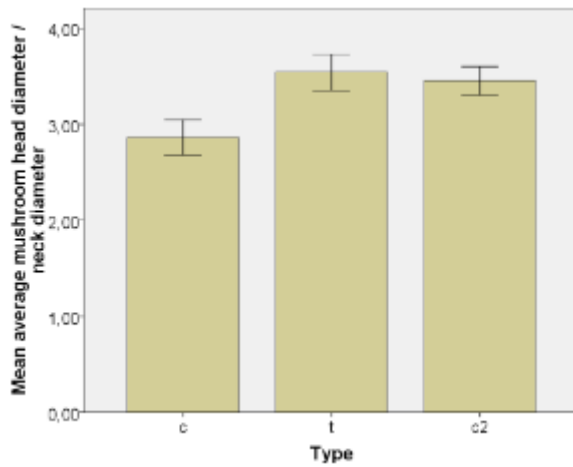

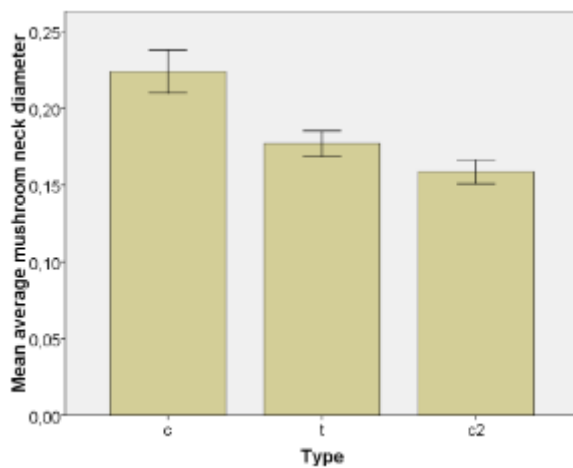**Figure 13: Mushroom head/neck diameter per type**

Figure 14: Mushroom neck diameter per type

Control vs treatment	t	df	Sig. (2-tailed)	Mean difference	Std. error difference
Mushroom ratio	-3,545	18,903	0,002	-0,11416	0,03221
Stubby ratio	4,205	14,765	0,001	0,22685	0,05395
Thin ratio	-2,764	19,465	0,012	-0,11269	0,04077
Spine density	-0,359	16,327	0,724	-0,10592	0,29476
Mushroom head/neck	-2,563	19,894	0,019	-0,67946	0,26506
Mushroom neck	2,890	15,022	0,011	0,04696	0,01625

Table 4: Independent T-test results of control group vs. treatment group

Control2 vs treatment	t	df	Sig. (2-tailed)	Mean difference	Std. error difference
Thin ratio	1,898	16,767	0,075	0,07138	0,03761
Mushroom head/neck	0,374	17,993	0,713	0,9010	0,24120
Mushroom neck	1,612	17,594	0,125	0,01836	0,1139

Table 5: Independent T-test results of second control group vs. treatment group

Datamining with Weka

We did data analysis with Weka for the 2 class problem, consisting of only the control and treatment groups dendrites, and the 3 class problem which also includes the 5 week old control group. We describe the results of a number of different methods of analysis that the Weka package offers.

Attribute selection by Information Gain

In general terms, the expected information gain is the change in information entropy, a measure of the uncertainty associated with a random variable, from a prior state to a state that takes some information (23). This information gain can be used as a measure of attributes functioning as a class predictor. For both the 2 class and the 3 class problems the same four attributes appear to have a high information gain. This suggests that each of these four attributes can be used alone as class predictors.

Attribute	Information gain
Stubby/spine ratio	0.618
Mushroom head/neck ratio	0.502
Mushroom/spine ratio	0.445
Mushroom average neck diameter	0.432

Table 6: Information gain per attribute for the 2 class problem

Attribute	Information gain
Stubby/spine ratio	0.496
Mushroom average neck diameter	0.418
Mushroom head/neck ratio	0.398
Mushroom/spine ratio	0.365

Table 7: Information gain per attribute for the 3 class problem

Subset analysis

A subset analysis algorithm is used to find the combination of attributes that together have a high information gain. The best subset for both the 2 class and the 3 class problem as found by the algorithm consist of exactly the same four attributes as described above. This suggests that there is not enough correlation between any of the predictors to be able to discard one of the predictors, which means that all four predictors are useful in further analysis.

Visualization

The attributes as found by WEKA can be visualized in a scatter diagram in which two attributes are combined. These scatter diagrams can be used to get a general overview of the results. The different research groups are depicted as follows:

Research group	Color
Control (C)	Blue
Treatment (T)	Red
Second control (C2)	Green

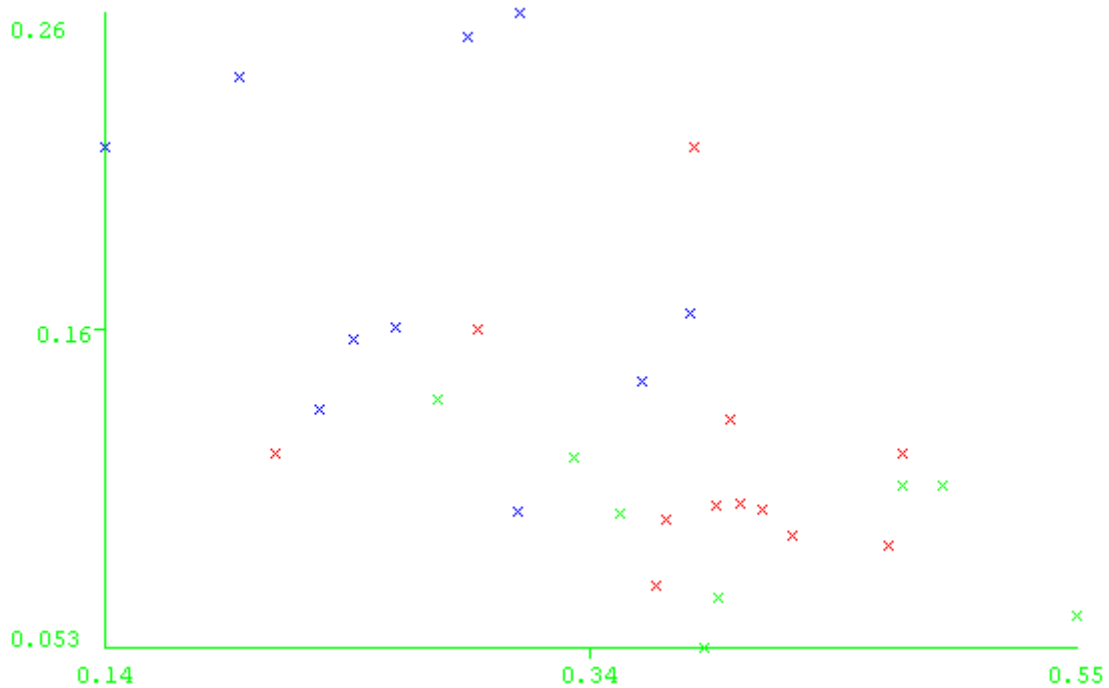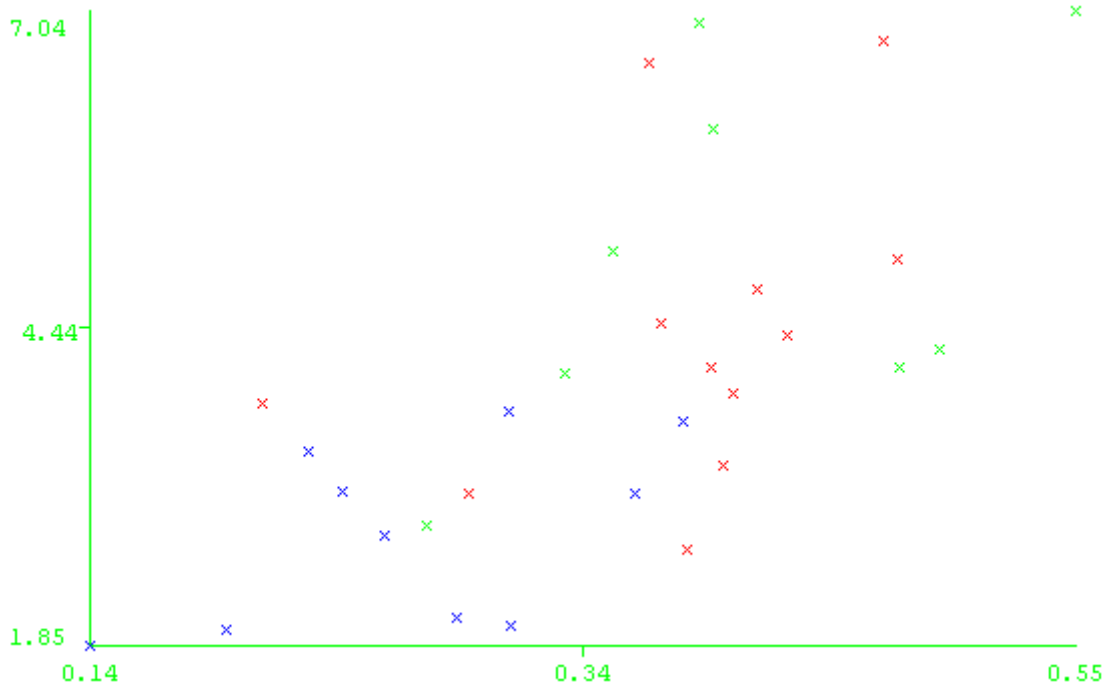**Figure 15: Mushroom/spine ratio (x) vs. mushroom average neck diameter (y)**

Figure 16: Mushroom/spine ratio (x) vs. mushroom head/neck ratio (y)
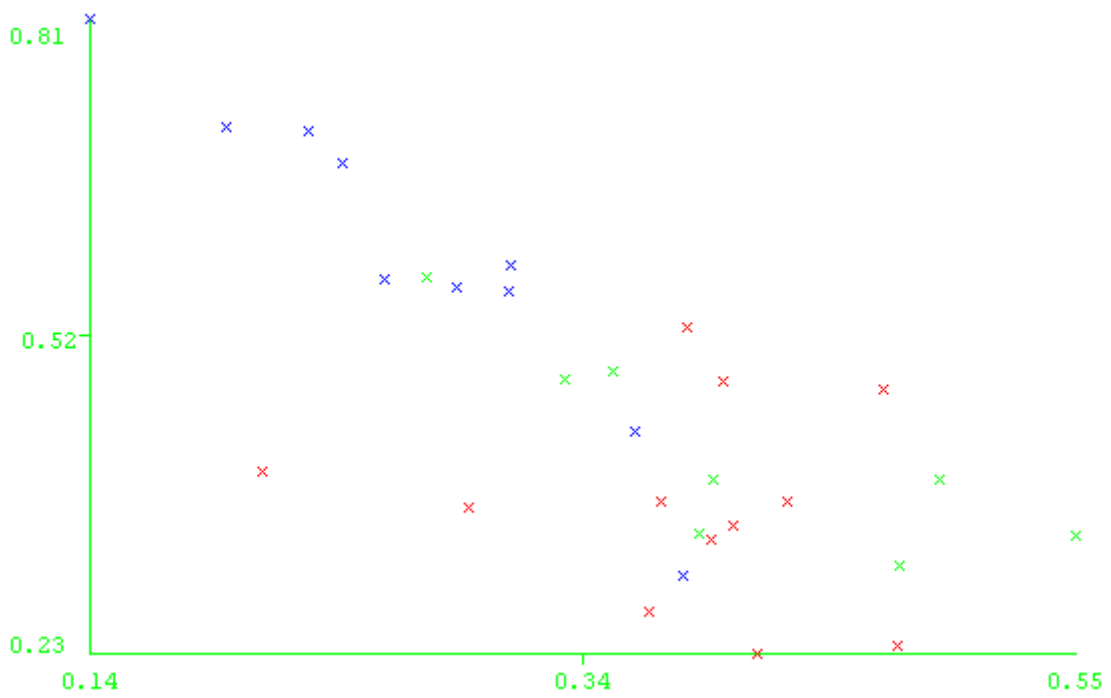

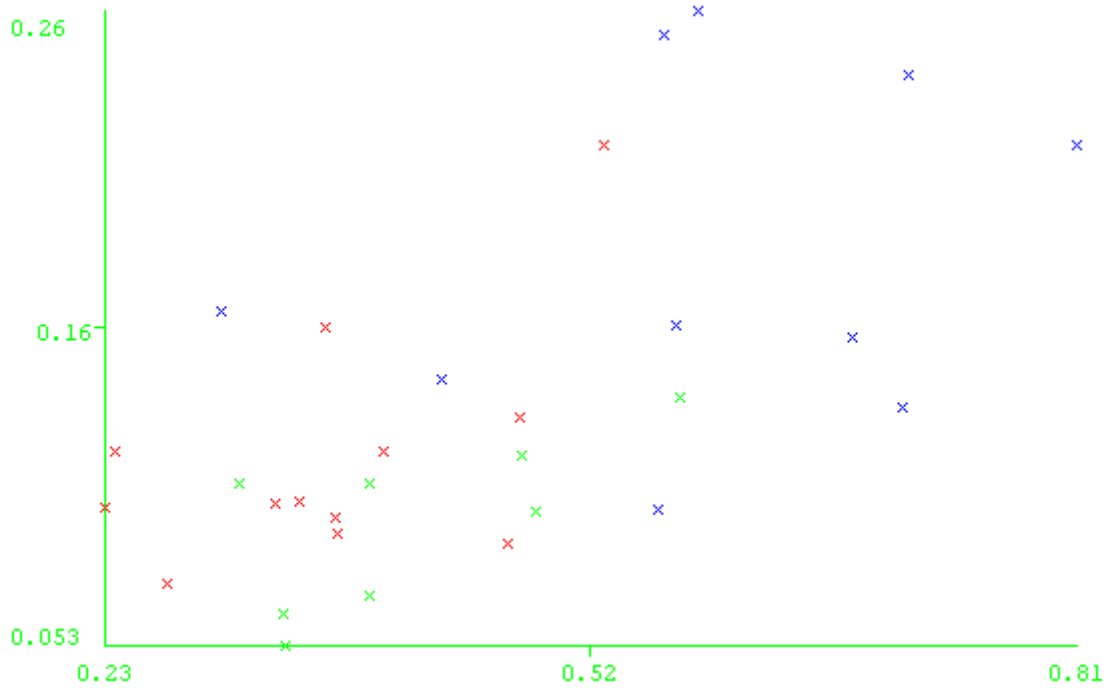**Figure 17: Mushroom/spine ratio (x) vs. stubby/spine ratio (y)**

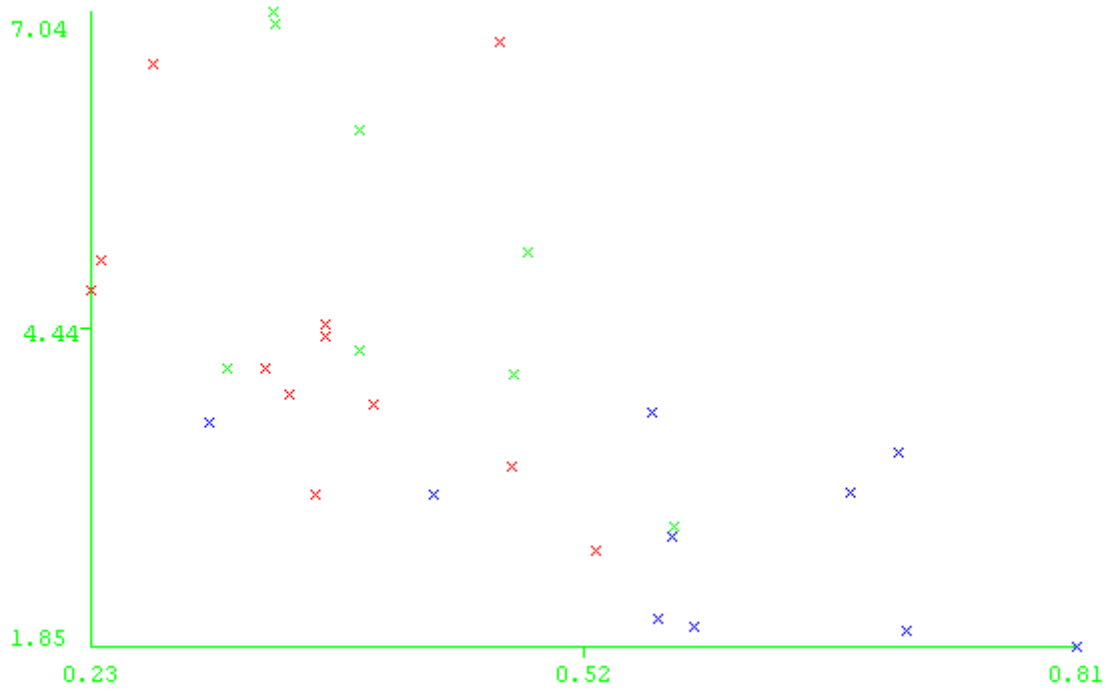Figure 18: Stubby/spine ratio (x) vs. mushroom average neck diameter (y)

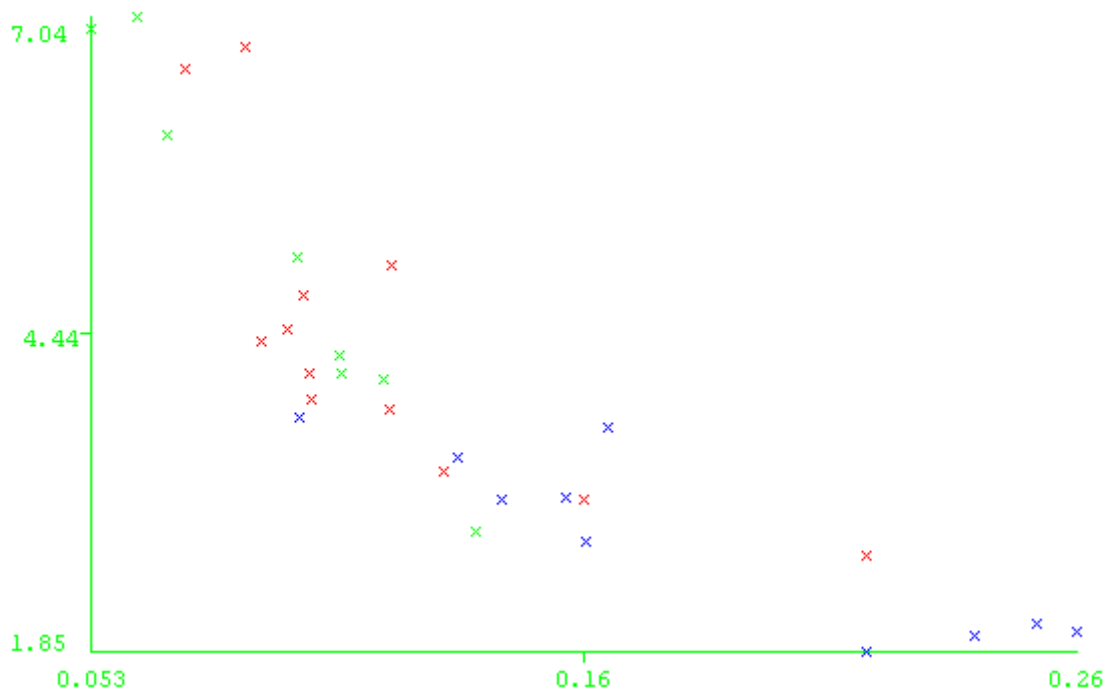Figure 19: Stubby/spine ratio (x) vs. mushroom head/neck ratio (y)

Figure 20: Mushroom average neck diameter (x) vs. mushroom head/neck ratio (y)

Cluster analysis

To do clustering analysis we have used a simple k-Means algorithm. The clustering algorithm defines clusters of dendrites by their attributes without using any information on the class of the dendrites. We used it to divide the instances of the 2 class problems into two clusters and the instances of the 3 class problem into three clusters. The classes are then mapped on to the clusters in the best way possible. We performed the clustering both using all attributes and using only the four top predictors, because removing attributes that are not good class predictors could have a positive effect on the success rate.

The results for the 2 class problem suggest a clear divide between the control group and the treatment group.
The results for the 3 class problem show that there are no differences found between the treatment and the five week old control group. Clusters that contain a high amount of treatment samples also contain a high amount of five week old control samples and vice versa. We also see that the control group and the five week old control group are mostly separated. Again we see a clear divide between the control and the treatment group.

2-class

class/cluster	0	1
C	6	4
T	1	11

Cluster 0 ← c
Cluster 1 ← t
Incorrectly clustered instances: 5/22 (23%)

2-class with only 4 top predictors

class/cluster	0	1
C	8	2
T	3	9

Cluster 0 ← c
Cluster 1 ← t
Incorrectly clustered instances: 5/22 (23%)

3-class

class/cluster	0	1	2
C	1	6	3
T	4	1	7
c2	2	1	5

Cluster 0 ← t
Cluster 1 ← c
Cluster 2 ← c2
Incorrectly clustered instances: 15/30 (50%)

3-class with only 4 top predictors

class/cluster	0	1	2
C	5	3	2
T	0	1	11
c2	1	0	7

Cluster 0 ← c
Cluster 1 ← No class
Cluster 2 ← t
Incorrectly clustered instances: 14/30 (47%)

Classifier with experimenter

We have run several different classification algorithms and compared their results to find which algorithm performs best. The four algorithms that we used are:

- **ZeroR**, which classifies everything as part of the majority class, without using any of the attributes.
- **J48**, which creates a decision tree.
- **Naive Bayes**, based on probability models and decision rules.
- **IB1**, also known as the nearest neighbor algorithm.

We included the ZeroR algorithm for comparison reasons, if the performance of a classifier is close to the performance of the ZeroR classifier then its performance is considered poor.

We did both a 10-fold cross validation and a 66% training, 33% test set division. Both are repeated a 100 times and results are averaged. The results show that all three algorithms are able to build a working classifier for the 2 class problem, as they perform significantly better than the ZeroR classifier. However, they are imperfect, with a succes rate around 70%. The performance of the classifiers for the three class problem are lower. The best algorithm here is IB1, with a succes rate around 56%, where the ZeroR has a succes rate around 40%.

10-fold training, 100 repetitions	ZeroR	J48	NaiveBayes	IB1
2-class	53.33	72.43	75.62	68.33
3-class	40.00	37.20	47.27	57.40

66% training set, 100 repetitions	ZeroR	J48	NaiveBayes	IB1
2-class	53.72	72.43	69.16	69.34
3-class	38.83	45.58	48.98	55.91

Table 8: Success rates per problem and algorithm

Workflow overview
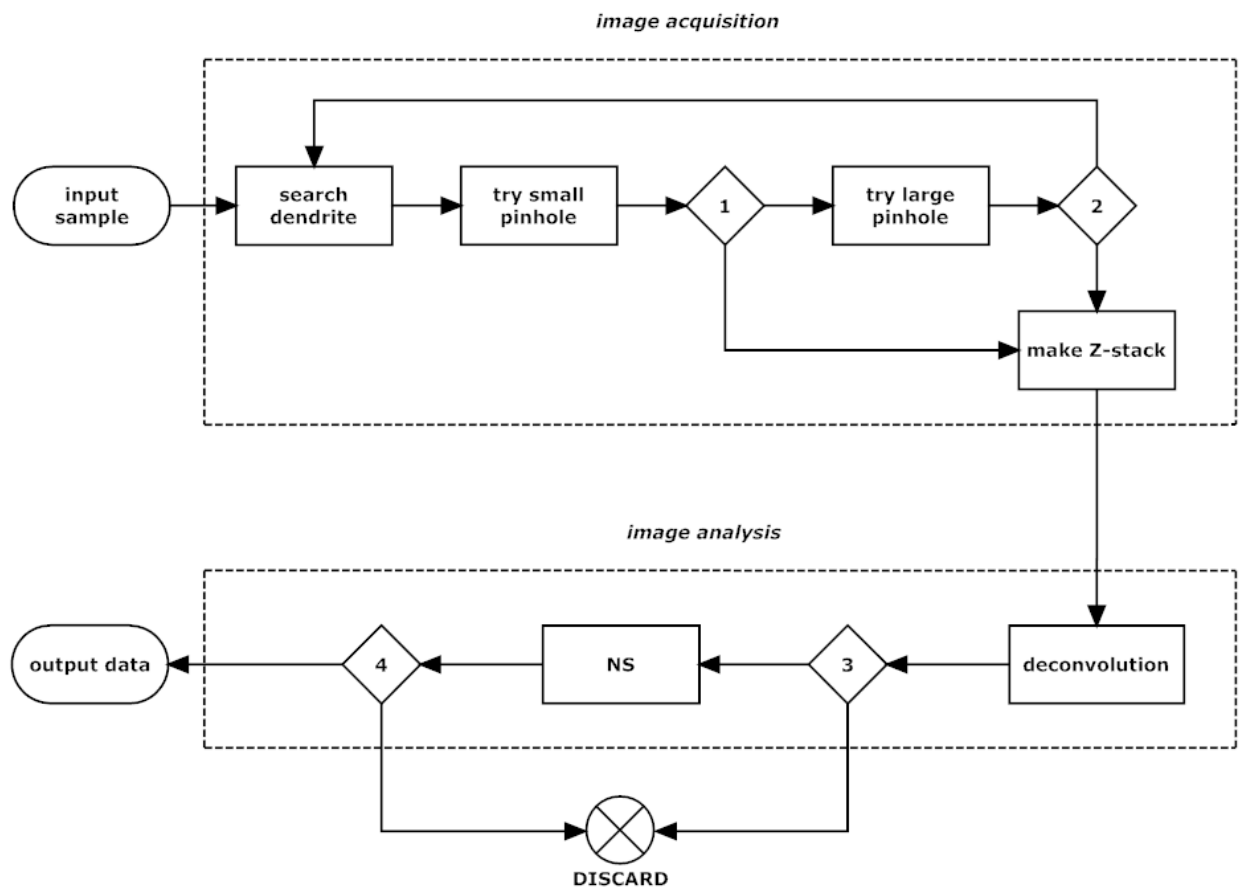
Figure 21: Workflow overview

#	condition	true	false
1	sufficient signal strength	go to 'make Z-stack'	go to 'try large pinhole'
2	sufficient signal strength	go to 'make Z-stack'	go back to 'search dendrite'
3	successful deconvolution	go to 'NS'	discard
4	successful NS analysis	export data	discard

Table 9: Decisions in the workflow overview

Starting with an input sample, the first step is finding the hippocampus by controlling the microscope manually using the 20x lens. Then a suitable dendrite must be found using the 60x lens with oil immersion. The small pinhole will be tried first by making a test slice of the dendrite using the software mode. If the signal strength is sufficient, the Z-stack can be made. If not, the large pinhole has to be tried (decision #1). If the signal strength is still not good enough, another dendrite has to be searched for. Otherwise, the Z-stack can be made (decision #2). Making the Z-stack consists of finding the enclosing coordinates for a suitable dendrite segment and acquiring a Z-stack (3D image) using the microscope software. The resulting image is deconvolved using the Huygens software with predetermined settings. If the resulting image is of sufficient quality, it is used as input image for NS using predetermined settings. If not, the image is discarded (decision #3). Finally, if NS is able to succesful analyse the image data, the result is be exported for further processing. Otherwise, the image is discarded (decision #4).

Conclusion

The image analysis in this research is based on NS. The main challenge in using this software has shown to be that it requires high quality images in order to properly analyse the dendrites and the spines. We have developed a method of image acquisition that is aimed towards acquiring high quality images. This acquisition method has proven to be effective, with the majority of acquired images being suitable for use in NS. This method of image acquisition together with the use of deconvolution software and NS has proven to be very efficient in creating large quantities of morphological data on dendrites and spines.

Data analysis showed strong differences between the samples from the control and the treatment group. Both the amounts of different types of spines and the shapes of the mushroom spines differ strongly between the two groups. The differences that we found suggest that the samples from the treated group contain in general more developed spines than those from the control group.
The five week old control group showed similar differences to the one week old control group. These differences can be explained by the fact that the five week old control group is in a more developed state because of the difference in age.

Discussion

Analysing the dendrites was done in a semi-automated fashion. Not only by using software for automated image analysis, but also by processing all samples the same way, as the process overview of the result section indicates. In this way we aimed to minimize possible bias. Bias may still occur in several stages, as each time a decision in the workflow has to be made the resulting quality is subjectively judged. Bias can also occur when picking input samples, finding the hippocampus and searching for possible dendrites. Bias is largely created by the fact that the maximum resolution of the microscope is close to the resolution needed to analyse the spine structures, which makes it difficult to get images of sufficient quality. Because the developed method for analysing the data depends on this fact, bias will be present.

Some results in this research were significant, others were not. Spine density, for example, showed no significant differences between each group. Using more samples, one might conclude that besides the differences in spine type, also the amount of spines differ between each group. This may give some new insights into the maturation of spines of GR-knockdown dendrites.
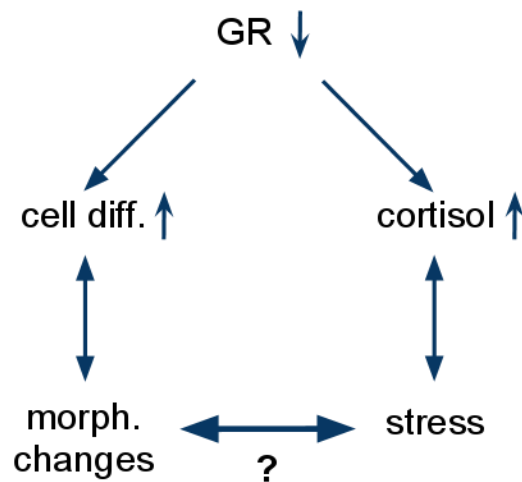

Figure 22: Implications of GR-knockdown

GR-knockdown will lead to increased levels of cortisol because of a deficient feedback of cortisol and promotes neuronal cell differentation [12], [13]. Increased cell differentation will result in morphological changes and raised levels of cortisol will result in a stress reaction. Clinically, the GR-knockout mice will therefore show stressful behaviour. The question that remains is whether or not stressful behaviour can lead to morphological changes. To be sure the morphological changes are only induced by the GR knockdown, one should also do research on the isolated stress factor.

Because it is believed that abnormal formation of dendritic spines is related to learning disorders [2], a better understanding of the underlying morphological changes of such learning disorders might help us to find treatments.

References

1. [Online] http://en.wikipedia.org/wiki/Neurons.
2. *A neurodevelopmental approach to specific learning disorders.* **Whitmore, Kingsley.** s.l. : Cambridge University Press, 1999, pp. 29-32.
3. **Mildner.** [book auth.] Taylor. *Cognitive Neuroscience of Human Communication.* 2008, pp. 5-7.
4. *Development of neural circuits in the adult hippocampus.* **Li Y, Mu Y, Gage FH.** 2009, Curr Top Dev Biol.
5. *Synaptic plasticity, memory and the hippocampus: A neural network approach to causality.* **G. Neves, S.F. Cooke and T.V. Bliss.** 2008, Nature Reviews Neuroscience, pp. 65-75.
6. *Adult neurogenesis produces a large pool of new granule cells in the dentate gyrus.* **Cameron HA, McKay RD.** 435 (4), 2001, J Comp Neurol, pp. 406-17.
7. *Adult neurogenesis and neural stem cells of the central nervous system in mammals.* **Taupin P, Gage FH.** Sep 2002, J Neurosci Res.
8. *Mammalian neural stem cells.* **Gage, F.H.** 2000, Science 287, pp. 1433-1438.
9. *Neural stem cells from adult hippocampus develop essential properties of functional CNS neurons.* **H.J. Song, C.F. Stevens and F.H Gage.** 2002, Nat. Neurosci. 5, pp. 38-445.
10. *In vivo fate analysis reveals the multipotent and self-renewal capacities of Sox2(+) neural stem cells in the adult hippocampus.* **H. Suh, A. Consiglio, J. Ray, T. Sawai, K.A. D'Amour and F.H. Gage.** 2007, Cell Stem Cell 1, pp. 515-528.
11. *Antiglucocorticoids, neurogenesis and depression.* **Fitzsimons CP, van Hooijdonk LW, Morrow JA, Peeters BW, Hamilton N, Craighead M, Vreugdenhil E.** Feb 2009, Mini Rev Med Chem., pp. 249-64.
12. *The microtubule-associated protein doublecortin-like regulates the transport of the glucocorticoid receptor in neuronal progenitor cells.* **Fitzsimons, C.P., et al., et al.** 22, 2008, Mol Endocrinol, pp. 248-62.
13. *Lentivirus-mediated transgene delivery to the hippocampus reveals sub-field specific differences in expression.* **van Hooijdonk, L.W., et al., et al.** 10, 2, 2009, BMC Neurosci.
14. *Automated Three-Dimensional Detection and Shape Classification of Dendritic Spines from Fluorescence Microscopy Images.* **Rodriguez A, Ehlenberger DB, Dickstein DL, Hof PR, Wearne SL.** 3 (4), 2008, PLoS ONE.
15. [Online] http://en.wikipedia.org/wiki/Data_mining.
16. *Nikon EZC1 Manual.*
17. [Online] http://www.svi.nl/.
18. *Huygens Essential Manual.*
19. [Online] http://www.cs.waikato.ac.nz/ml/weka/.
20. [Online] http://en.wikipedia.org/wiki/Weka.
21. *Do thin spines learn to be mushroom spines that remember?* **Bourne J, Harris KM.** 17(3), June 2007, Curr Opin Neurobiol., pp. 381-6.
22. *Head, neck, and spines: a role for LIMK-1 in the hippocampus.* **Sarmiere PD, Bamburg JR.** 3;35(1), July 2002, pp. 3-5.
23. **I.H. Witten, E. Frank.** *Data Mining.* pp. 93-96.